2009

Phasic and tonic modes of depolarization-exocytosis coupling in β-cells of porcine islets of Langerhans

Stanley Misler
Washington University School of Medicine in St. Louis

Amelia M. Silva
Washington University School of Medicine in St. Louis

David Barnett
Washington University School of Medicine in St. Louis

Adam S. Dickey
Washington University School of Medicine in St. Louis

[Channels 3:2, 101-109; March/April 2009]; ©2009 Landes Bioscience

Research Paper

Phasic and tonic modes of depolarization-exocytosis coupling in β-cells of porcine islets of Langerhans

Stanley Misler,* Amelia M. Silva,† David Barnett‡ and Adam S. Dickey§

Departments of Internal Medicine & Cell Biology/Physiology; Washington University Medical Center; Saint Louis, MO USA

†Current address: Department of Biology and Environment; CITAB; University of Trás-os-Montes e Alto Douro; Vila Real, Portugal; ‡Current address: Medical Scientist Training Program; University of Chicago Medical Center; Chicago, IL USA; §Current address: Department of Biomedical Engineering; Saint Louis University; St. Louis, MO USA

Abbreviations: $[cAMP]_i$, cytosolic cAMP concentration; PSS, physiological saline solution; $[Ca^{2+}]_i$, cytosolic $[Ca^{2+}]$; QREs, amperometrically measured quantal release events; ΔC_m, membrane capacitance change

Key words: β-cell exocytosis, *phasic exocytosis*, *tonic exocytosis*, immediately releasable pool, highly calcium sensitive pool

In response to depolarizations that open voltage dependent Ca^{2+} channels single porcine β-cells display heterogeneous time courses of exocytosis. Some cells display *phasic exocytosis* that is triggered by individual or short burst of action potentials typically characteristic of glucose-induced electrical activity or brief voltage clamp depolarization. Other cells, singularly or additionally, display *tonic exocytosis* that (i) is triggered during prolonged (up to seconds-long) depolarizations to voltages (-30 to -20 mV), and (ii) coincides with rises in global cytosolic $[Ca^{2+}]$ >500 nM. We suggest that *tonic exocytosis* (i) likely results from a recently described pool of granules that is more Ca^{2+} sensitive and less co-localized with voltage-sensitive Ca^{2+} entry channels than that contributing to *phasic exocytosis* and (ii) helps tune exocytosis to glucose-induced electrical activity when the latter consists of spike activity followed by intervals of plateau depolarization to nearly -20 mV.

Introduction

Real-time single cell assays of depolarization-exocytosis coupling in pancreatic islet β-cells became available in the early 1990s with precise measurement of membrane capacitance (C_m) tracking membrane surface area, and local electrochemical (amperometric) detection of synchronized or quantal release of preloaded serotonin (by oxidation) or endogenous insulin (by reduction).[1-6] From the first of these experiments a "fast-on, fast off" mode of exocytosis was evident as a step increase in membrane capacitance C_m immediately after the conclusion of a brief depolarization or as a barrage of quantal release events during the depolarization.[1-5] This *phasic exocytosis* appears to arise from a small pool of granules, sometimes, called the immediately releasable pool, whose members have a low Ca^{2+} affinity and appear to be docked near clusters of high voltage activated Ca^{2+} channels.[4,6] This exocytosis may account for much of the first phase of glucose induced insulin release from perifused islets.[5] However, other records dating back to the same vintage, clearly show that longer depolarizations, especially when applied as a train, produce a "slower-on, slower off" mode of exocytosis monitored as creep-wise increase in C_m and persistence of amperometric discharge lasting up to seconds after the end of the depolarization.[2,7-10] This *tonic exocytosis*, which has received much less attention, may arise from a more highly Ca^{2+} sensitive pool of granules docked at some distance from a cluster of Ca^{2+} channels. The significance of this component of exocytosis, prominent in human and canine β-cells,[8-10] to the time course of insulin release is still unclear.

In our recent survey of stimulus-secretion coupling in porcine β-cells we noted that different cells displayed distinct time course of exocytosis in response to repetitive depolarization. Largely *phasic exocytosis* is highly synchronized with brief voltage-dependent Ca^{2+} entry; largely *tonic exocytosis* occurs during and after a train of longer depolarizations; and a combination of *phasic* + *tonic exocytosis*.[11] We have used this preparation to characterize further these modes of exocytosis and consider their differential contribution to exocytosis driven by different patterns of electrical activity.

*Correspondence to: Stanley Misler; Box 8126/Renal Division; Department of Internal Medicine; Washington University Medical Center; St. Louis, MO 63110 USA; Tel.: 314.454.7719; Fax: 314.454.5126; Email: smisler@dom.wustl.edu

Submitted: 11/17/08; Revised: 01/15/09; Accepted: 01/16/09

Previously published online as a *Channels* E-publication: www.landesbioscience.com/journals/channels/article/7866

Results

Heterogeneity of depolarization-induced, Ca^{2+}-entry-dependent exocytosis from single porcine β-cells. Figure 1 illustrates the key features of the wide heterogeneity of time course of exocytosis displayed by voltage-clamped porcine β-cells. In *A(i)*, the three cells depicted all display similar baseline values of C_m (6.3–6.7 pF) as well as similar sized voltage-dependent Ca^{2+} currents ($I_{Ca(v)}$) in response to a single depolarization (occurring during the gaps in the C_m trace). In addition, all three cells display similar time courses of increases in cytosolic Ca^{2+} concentration,

$[Ca^{2+}]_i$, as well as similar total increases in C_m in response to identical trains of ten 200 ms depolarizations to +10 mV delivered at 1 Hz. However, all three cells display distinct time courses of exocytosis within the train. The cell depicted in the left panel displays "step-wise" increases in C_m, exclusively, with each ΔC_m step completed at the end of a depolarization. This likely signifies that granule fusion occurred during the interval of voltage-dependent Ca^{2+} entry. We shall call this mode of release *phasic exocytosis* in that it appears to be nearly synchronous with the depolarization. Note, however, that successive depolarizations, though increasing $[Ca^{2+}]_i$ to ever higher levels, produced progressively smaller C_m steps, suggesting rapid depletion of the pool (or diminution of the store) of granules from which this exocytosis was drawn.

In contrast, the cell depicted in the middle panel displays no recognizable C_m step in response to the first depolarization. However, after the second depolarization it begins to display a slow "creep-wise" increases in C_m (or C_m creep), meaning that the change in C_m largely occurs between depolarizations rather than during these stimulations. This suggests that the exocytosis starts some time into each depolarization and then continues after the depolarization is completed. The rate of C_m creep accelerates during the subsequent five depolarizations, then decelerates for the remaining of four depolarizations of the train and continued for 2–3 s beyond the end of the train. We shall call this less synchronous mode of discharge *tonic exocytosis* and suggest that it originates from a pool of granules that does not rapidly deplete and may even be transiently augmented during the depolarization train.

Last, the cell depicted in the right panel displays a combined pattern of C_m increase: the steps of C_m seen early in the train seem to deplete, while the creeps of C_m clearly begin with the third depolarization and increase over the next 3–4 depolarizations. We shall call this *phasic + tonic exocytosis.* As the distinct patterns of exocytosis occur in neighboring cells with similar diameter, similar $I_{Ca(v)}$s and similar buildups of $[Ca^{2+}]_i$, we shall suggest that these patterns of exocytosis represent intrinsic modes of operation of the exocytotic apparatus.

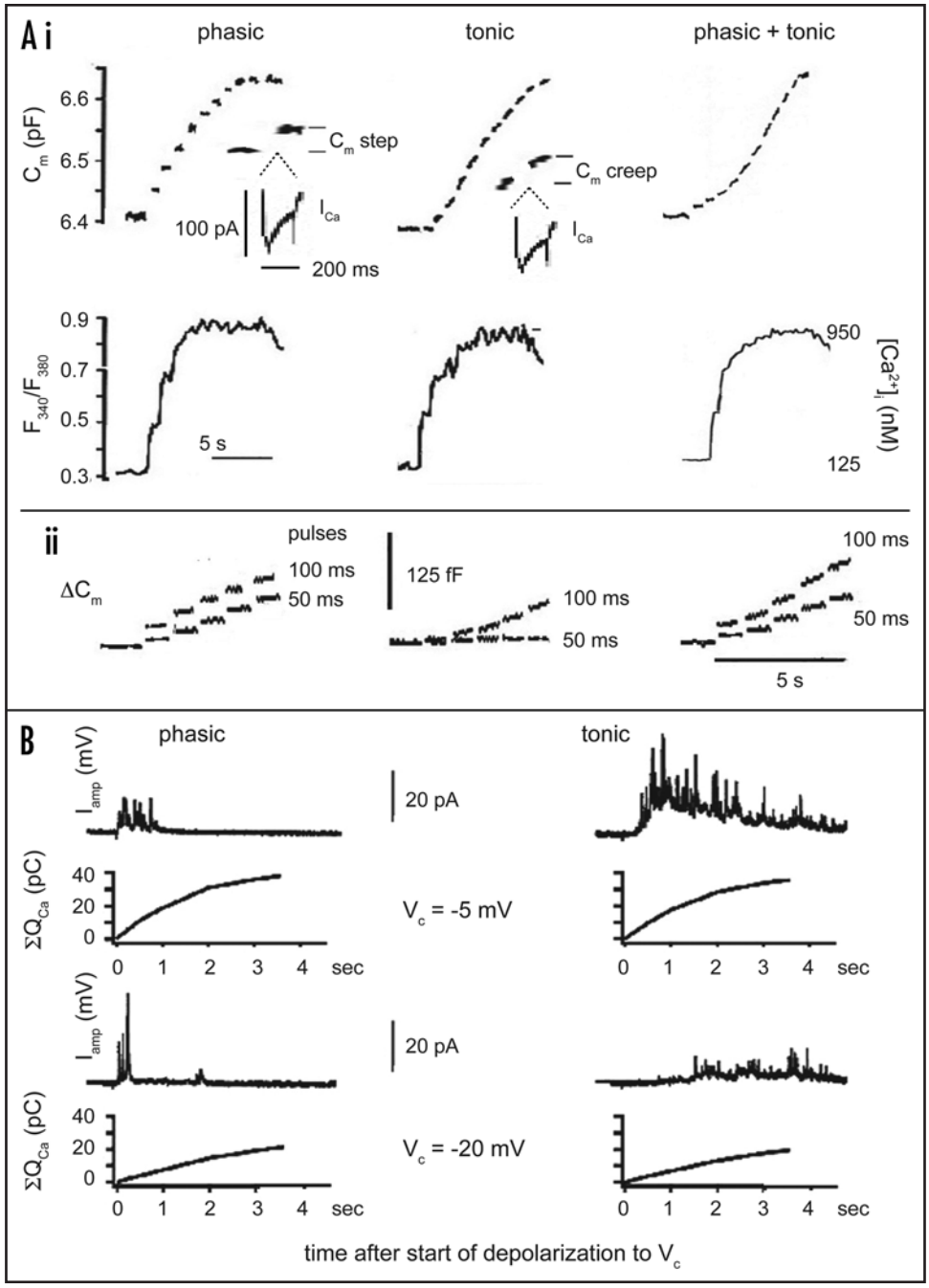

Figure 1. Cell-to-cell temporal heterogeneity of depolarization-exocytosis coupling in single porcine β-cells. (A(i)) distinct exocytotic patterns, *phasic, tonic* and *phasic + tonic exocytosis*, in three Fura-2AM pre-loaded, voltage-clamped cells selected for similar background C_m, total increases in C_m and $[Ca^{2+}]_i$ recorded during trains of ten, 200 ms depolarizations from -70 to + 0 mV. (A(ii)) *phasic exocytosis* is clearly evoked by single 50 ms depolarizing pulses to 0 mV, while *tonic exocytosis* requires several 100 ms pulses. (B) phasic vs. tonic components of exocytosis seen in amperometric recording of quantal release events from two 5-HT pre-loaded, voltage clamped cells during and after sustained 3.5 s depolarizations to indicated V_c (= -20 or -5 mV). The running integral of $I_{Ca(v)}$ over the duration of the depolarization is plotted as ΣQ_{Ca}.

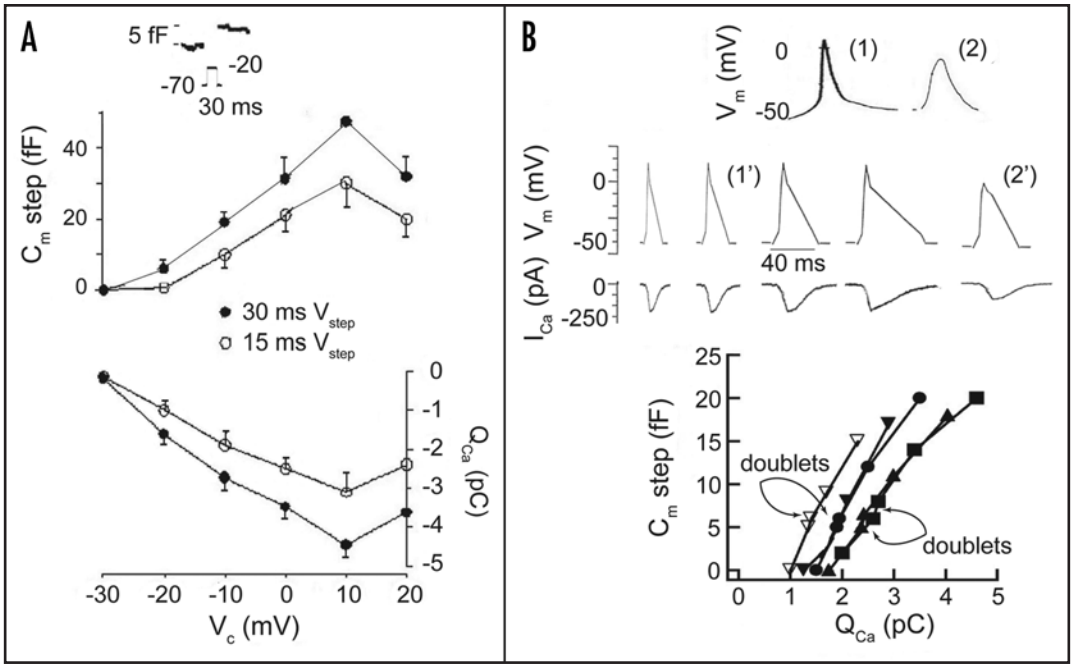

Figure 2. Minimal Ca entry for evoking phasic exocytosis. (A) dependence of *phasic exocytosis* (C_m step) on depolarization voltage V_c and Ca^{2+} entry (Q_{Ca}) at two lengths of depolarization, 15 and 30 ms. Under both conditions C_m steps peak at depolarizations to +10 mV where Q_{Ca} is maximal. (B) dependence of phasic exocytosis on Q_{Ca}s evoked by action potentials of widely varying shapes. Top row shows sample native APs recorded in current clamp mode with K^+-IS pipette. The second and third row presents a range of voltage clamp simulated APs using Cs^+-IS pipette, and Ca^{2+} currents (I_{Ca}s) they evoked in substituted PSS containing 8 mM glucose, 20 mM TEA-Cl and 0.5 mM TTX. APs labeled 1' and 2', most resemble the corresponding sample native APs 1 and 2. While the latter APs differ greatly in shape they evoke similar total Q_{Ca}s, the larger AP evoking a briefer but more intense Ca^{2+} entry, and the smaller AP evoking a less intense but more extended Ca^{2+} entry. The corresponding graph presents a summary of C_m vs. Q_{Ca} in five robustly secreting cells subjected to the range of the simulated APs shown. Each point represents the average of at least 4 trials separated by 20 s intervals. Arrows indicate the "doublet points" representing the effects of simulated APs 1' and 2'. In four of the five cells, simulated APs 1' and 2' were competent in evoking reliably measured increases in C_m of greater than or equal to 5 fF (i.e., 3-fold greater than baseline noise in these experiments).

To further explore each of the three exocytotic patterns *A(ii)* depicts typical capacitance traces recorded, in response to trains of five repetitive depolarization of two different pulse lengths (50 ms vs. 100 ms), from each of the cells presented in *A(i)*. Note that the cell identified as displaying *phasic exocytosis* exhibits an initial C_m step that increases with prolongation of depolarization; however C_m step responses to subsequent depolarizations depress. In contrast, the cell identified as exhibiting *tonic exocytosis* shows no C_m step response to individual 50 or 100 ms depolarizations, yet displays onset of C_m creep after the second (or third) 100 ms depolarization. Finally, note that the cell identified as displaying *phasic + tonic exocytosis* exhibits an apparent summation of the two effects.

In a complementary fashion, *B* demonstrates that similar heterogeneity of exocytosis is seen when discrete quantal release events (QREs) were monitored, by carbon fiber electrode amperometry, from 5-HT-preloaded, voltage-clamped cells. Shown here are amperometric traces from a pair of porcine β-cells, both of which display very similar baseline C_ms (left 6.3 pF vs. right 6.5 pF) and total Ca^{2+} entries (Q_{Ca} = the integrals of $I_{Ca(v)}$) over the durations of continuous 3.5 s depolarizations from -70 mV to either -20 or -5 mV. Also, both cells display similar voltage-dependence of total exocytosis, with the 15 mV increase in test depolarization producing at least a 4-fold increase in the total number of QREs. The cell in the left panel, labeled *phasic exocytosis*, commenced its quantal release as rapidly as 25 ms after onset of depolarization and then ceased to release by 2 s into the sustained depolarization. However, the cell in the right panel, labeled *tonic exocytosis,* commenced its quantal release at the earliest only after 200 ms of onset of depolarization, while continuing it, though at decreasing rate, for the entire 3.5 s of depolarization and then for ~1.5 s thereafter. This comparison suggests that in *phasic exocytosis* the entering Ca^{2+} sets off highly localized release from a small pool of immediately releasable granules likely docked near Ca^{2+} entry channels, while in *tonic exocytosis* the entering Ca^{2+} must accumulate and diffuse to reach and discharge a larger more dispersed pool of granules at some distance from the Ca^{2+} entry channels.

In total, of the 23 cells examined in one of the recording conditions shown here, six exhibited *phasic exocytosis* exclusively, seven *tonic exocytosis* exclusively, while ten showed combined *phasic + tonic exocytosis* pattern, in which it was possible to extinguish the phasic component by repeating the depolarization train within 20–30 s of the prior train.

Minimal conditions for phasic exocytosis (nearly synchronous with duration of depolarization) vs. tonic exocytosis (slower-to-start and slow-to-stop). Figure 2 illustrates two sets of experiments designed to quantify the minimal Ca^{2+} entry needed to provoke detectable quantal release and determine whether single action potentials seen in porcine β-cells are capable of providing this.

First, as shown in (A), robustly secreting porcine β-cells were tested with single, brief (20–35 ms) depolarizations applied in random sequence at 20–30 s intervals. Note that the amplitude of resultant C_m steps was clearly voltage-dependent and closely paralleled Q_{Ca}. Little if any increase in C_m was seen at voltages negative to -25 mV; however the amplitude of C_m steps increased sharply with increasing depolarization, peaking at +10 mV, where Q_{Ca} is maximal. Thereafter, the amplitude of C_m steps sharply decreased with larger depolarization. While 15 ms-long depolarizations to -20 mV evoked no detectable increase in C_m over 10 trials, 15 ms-long depolarizations to -10 mV, which provoked 2-fold greater increases in Ca^{2+} entry, evoked highly reproducible steps of C_m averaging 20 fF, or roughly equivalent to the fusion of 7–10 insulin granules. Increasing the duration of depolarization to 30 ms resulted in readily detectable C_m steps even at -20 mV, with 7/10 such depolarization trials producing C_m steps at least 5 fF in amplitude. In a set of six β-cells, in which we had previously recorded action potentials evoked by 12 mM glucose under current-clamp conditions, we noted that at least 70% (108/168) of the action potentials spent at least 30 ms at potentials equal or positive to -20 mV (i.e., -20 to +10 mV). This suggested that in robustly secreting β-cells the majority of single action potentials might be capable of evoking detectable quantal release.

Second, to test this hypothesis more directly, in several β-cells we investigated the effectiveness of various simulated action potential (AP) waveforms, applied as complex voltage-clamp sequences, in evoking increases in C_m. Examination of effects of changes in action potential shape on calcium currents and transmitter release has proven a useful tool for examining synaptic transfer curves across central synapses and depolarization-exocytosis coupling at peripheral nerve terminals.[14] In *B*, the top row presents traces (1) and (2), representing the extremes of shape of glucose-provoked APs recorded from porcine β-cells; the second row presents a range of voltage-clamp simulated APs, including those resembling the sample native APs, here labeled (1') and (2'); the third row presents the corresponding Ca^{2+} currents ($I_{Ca(v)}$s) the simulated APs evoke. Of note is that $I_{Ca(v)}$s occur largely during the decay phase of the action potential and that for a given peak depolarizing voltage, the longer the decay phase, the longer the $I_{Ca(v)}$ duration and the more intense the total Ca entry, Q_{Ca}. Also, simulated APs of different waveforms (e.g., 1' and 2') can evoke $I_{Ca(v)}$s of quite differ shapes but of very similar total Q_{Ca}s. The graph at the bottom of *B* presents a summary of C_m vs. Q_{Ca}compiled from records of five robustly exocytosing cells subjected to the range of the simulated APs shown. In four of the five cells, simulations of the sample APs were competent in evoking reliably measured increases in C_m.

Figure 3 illustrates a set of experiments designed to test the range of global $[Ca^{2+}]_i$ needed to evoke *tonic exocytosis* and to compare this with the range of global $[Ca^{2+}]_i$ achieved during plateau depolarizations. In *A,* repetitive 50 or 100 ms depolarizations to -15 mV were applied to Fura-2AM-preloaded cells displaying both phasic and tonic components of exocytosis. Tonic exocytosis, characterized by the "creep-wise" increase in C_m, though only occasionally seen late into a train of 50 ms pulses, was routinely evident by the third or fourth pulse within a train of

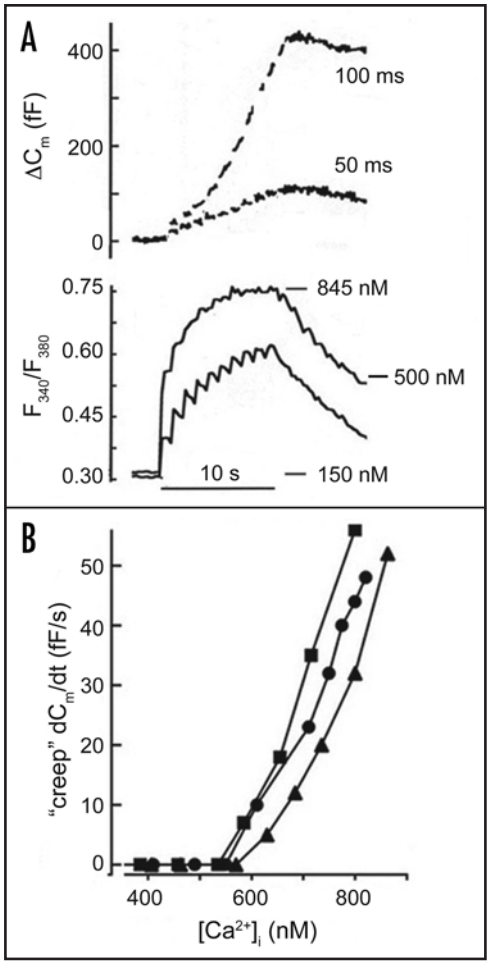

Figure 3. Minimal Ca entry and increase in cytosolic Ca necessary to evoke tonic exocytosis. (A) shows two different patterns of increase in C_m and $[Ca^{2+}]_i$ recorded from a Fura 2-AM-loaded cell during trains of 10 depolarizations (50 vs. 100 ms in duration) to -15 mV. Note that the train of 100 ms-long depolarizations evokes a continuous increase in C_m at $[Ca^{2+}]_i$ >500–600 nM. (B) shows that when tabulated for a set of three cells, including that depicted in the data traces in A (filled circles), the rate of C_m increase (dC_m/dt) displays a supralinear dependence on $[Ca^{2+}]_i$ at $[Ca^{2+}]_i$ >500–600 nM.

100 ms pulses. The appearance of tonic exocytosis coincided with rises in $[Ca^{2+}]_i$ to levels exceeding an estimated value >500 nM, in spite of little evidence of C_m steps. However, as is apparent in *B*, the rate of C_m creep (creep dC_m/dt), measured as the slope of the C_m curve, increased steeply as a supralinear function of $[Ca^{2+}]_i$ over the range 500–1,000 nM. As shown immediately below, this correlates well with the range of $[Ca^{2+}]_i$ measured during the intermittent plateau depolarizations that develop in many porcine β-cells during prolonged glucose-induced depolarization.

Evidence for plateau depolarization—type electrical activity to support sustained Ca entry and tonic exocytosis. In current-clamped, Fura-2 loaded porcine β-cells elevation of $[glucose]_o$ to 10–12 mM results, within minutes, in the appearance of (i) single action potentials that give rise to nearly simultaneous spikes of

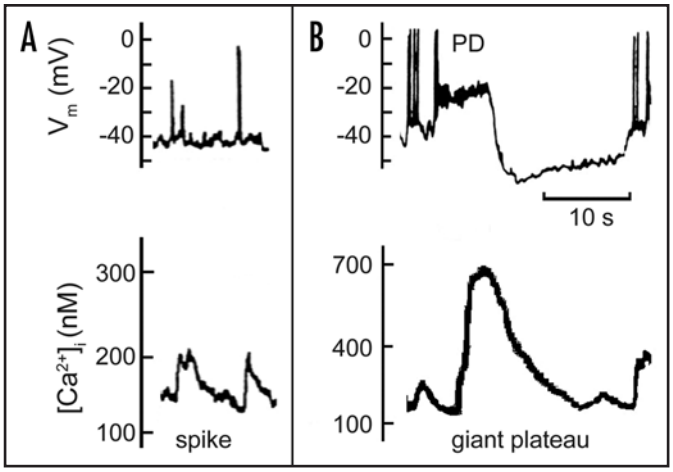

Figure 4. Two patterns of glucose-induced electrical activity and rises in $[Ca^{2+}]_i$. Simultaneous recording of V_m (*upper traces*) and cytosolic $[Ca^{2+}]$, ($[Ca^{2+}]_i$), (*lower traces*) at two intervals during exposure to 12 mM glucose. In (A) recorded 5 min after increasing $[glucose]_o$ from 2 to 12 mM, note that trains and even single action potentials evoke small transient rises in $[Ca^{2+}]_i$ from a nearly stable baseline of ~115 nM. In (B) recorded 12 min after increasing $[glucose]_o$ from 2 to 12 mM, note the appearance of a seconds-long plateau depolarization (PD) to ~-20 mV, which evokes a large transient rise in $[Ca^{2+}]_i$ to between 500 and 1,000 nM, here called a giant plateau. Cessation of the PD is followed by an after-hyperpolarization of V_m towards its resting value in baseline $[glucose]_o$,over which time the giant plateau slowly decays.

increases in $[Ca^{2+}]_i$ and (ii) clusters of APs that give rise to more prolonged bursts increases in $[Ca^{2+}]_i$. This coupling of action potential and $[Ca^{2+}]_i$ transient activitymay lastfor the duration of the cells' exposure to elevated $[glucose]_o$ (see Fig. 1D in companion paper and Fig. 4A here). However, with exposures to elevated $[glucose]_o$ for greater than 8–10 min it is not unusual for intermittent *plateau depolarizations* (PD), lasting from 10 to 55 seconds at a V_m between -25 and -15 mV, to arise after a train of action potentials. These PDs bring $[Ca^{2+}]_i$ to values between 500 and 1,000 nM (see Fig. 4B). We call these sustained $[Ca^{2+}]_i$ transients *giant plateaus.* PDs end in abrupt repolarizations of V_m to -55 to -60 mV lasting 10 to 15 s and accompanied by recovery of $[Ca^{2+}]_i$ to a baseline of 100 to 200 nM. Thereafter V_m depolarizes to between -45 and -40 mV and the cell resumes its firing of irregular action potentials accompanied by spike or burst-like $[Ca^{2+}]_i$ transients.

We observed these PD/giant plateau combinations in 9/12 current-clamped, Fura-2 loaded porcine β-cells whose responses to elevated $[glucose]_o$ were monitored for longer than 9 min. In these cells, in the interval between 7–15 min in $[glucose]_o$ = 12 mM, the fraction of time a cell spent in the PD/giant plateau mode was 3–12%.

Increases in $[cAMP]_i$ enhance phasic exocytosis and reveal tonic exocytosis. In our companion study,[11] confirming prior studies of β-cells in other species[15,16] we showed that augmenting $[cAMP]_i$, either by applying a membrane permeant derivative or by stimulating adenylate cyclase, via binding a G-protein coupled receptor for glucagon or glucagon-like intestinal peptide 1 (GLP-1), increased single cell insulin granule exocytosis, measured as ΔC_m. Often either maneuver produced little or no enhancement of depolarization-induced calcium entry. In Figure 5 we have re-examined this finding in porcine β-cells in the light of our dissection of phasic from tonic modes of depolarization-induced exocytosis. Panel A presents data from a single cell demonstrating that raising $[cAMP]_i$ by exposure of cells previously untreated with forskolin to the membrane permeable analog 8-CPT-cAMP, enhances phasic exocytosis (C_m steps immediately following the initial 2–3 depolarizations in a train), as well as recruits tonic exocytosis (C_m creeps after the remaining depolarizations in the train) not at all appreciated under control conditions. Summarizing data from five cells, Panel *B* demonstrates that, on average, a 6 min incubation of forskolin-naïve cells with 8-CPT-cAMP produces on average a 3-fold increase phasic exocytosis (as defined above) as well as a near 20-fold increase tonic exocytosis (as defined above), as compared with control conditions.

Discussion

Many porcine β-cells display a "fast on-fast off" pattern of exocytosis that is synchronous with depolarization. This *phasic exocytosis* closely resembles the major mode of secretion reported in varying detail in rodent β-cells, from the inception of single cell assays of exocytosis and thought to contribute to the bulk of first phase glucose-induced insulin secretion from these cells.[1-6] Here we demonstrate that porcine β-cells display *phasic exocytosis* in response to single brief depolarizations to clamping potentials positive to -20 mV; it consists of a burst of quantal release events (QREs) during the effective depolarization and step increase in C_m immediately after cessation of the depolarization, with the intensity of the QRE burst and the magnitude of the step increase in C_m increasing with increasing Ca^{2+} entry. *Phasic exocytosis* is also seen during a train of depolarizations; however, under these conditions both the burst of QREs *during*, and the step increase in C_m *following*, each interval of depolarization *decreases* with pulse repetition, even as the average cytosolic $[Ca^{2+}]$ progressively *increases*. The latter suggests that the pool of granules contributing to *phasic exocytosis*, though almost immediately useable, is of limited capacity and hence rapidly depleting. Application of cell attached patch recording to mouse β-cells has shown that the opening of 1–2 Ca^{2+} channels results, within a few milliseconds, in a small (1.5–2.5 pF) step increase in C_m consistent with the fusion of a 250 nm diameter insulin granule with the plasma membrane.[4,5] In the latter cells, the small pool of ~50–100 insulin granules contributing to *phasic exocytosis* is also released when the submembrane $[Ca^{2+}]$ is raised to the level of >10 μM by vigorous flash photolysis of caged Ca^{2+} compound previously injected into the cytoplasm.[6] This "immediately releasable pool" (IRP) of granules is likely localized very near the internal mouths of a small group of Ca^{2+} channels, since at larger distances from the channels the amplitude of the Ca^{2+} micro-domain would rapidly fall below the threshold concentration of >10 μM required for triggering release of granules comprising this pool.

However, the majority of porcine β-cells also display, either alone or in combination with the *phasic exocytosis*, a "slow on-slow off" pattern of exocytosis, which we call *tonic exocytosis*. The latter consists of the steady appearance of quantal release events,

asynchronous with depolarization and accompanied by a progressive, "creeping" increase in C_m. Both the quantal release events and the increase in C_m begin as late as hundreds of ms into, and continue for up to several seconds after cessation of, a prolonged depolarization, to voltages positive to -30 mV. *Tonic exocytosis* first appears after total Ca^{2+} entry increases global $[Ca^{2+}]_i$ to > 500–600 nM, as measured by slowly responding Ca^{2+} indicator dyes such as Fura compounds. At higher $[Ca^{2+}]_i$s, the rate of this mode of exocytosis rises steeply. We assume that the average $[Ca^{2+}]_i$, measured by imaging the cytoplasm globally, applies to the region immediately beneath the plasma membrane because in similarly sized adrenal chromaffin cells admitting similar Ca^{2+} currents, confocal microscopy reveals that $[Ca^{2+}]_i$ reaches a uniform global level after ~200 ms depolarization to voltages (-10 to 0 mV) where Ca^{2+} current is near maximal.[18] This tonic mode of exocytosis was clearly present in the C_m responses to trains of depolarization recorded in early experiments with rodent β-cells, and was massively enhanced when external Ca^{2+} was replaced with Sr^{2+} or Ba^{2+}.[2,7] However, tonic exocytosis has merited little comment or discussion and its physiological significance has only been considered in recent literature on human β-cells.[8-10]

In contrast to phasic exocytosis, if the insulin granules contributing to tonic exocytosis constitute a discrete pool, it is likely that its member granules are located far from Ca^{2+} channels and have a much higher Ca^{2+} sensitivity. Ca^{2+} entering the cell via Ca^{2+} channels would need to (i) diffuse a longer distance, as well as (ii) avoid capture by both fixed and diffusible cytosolic Ca^{2+} buffers, to reach the release trigger sites associated with these granules. As initial Ca^{2+} entry would need to saturate these cytosolic buffers before sufficient Ca^{2+} were able to bind to granule trigger sites, onset of tonic release would be delayed by as long as hundreds of milliseconds after the onset of depolarization, as compared with phasic release, where the trigger is the high intensity burst. Recently, a novel component of the so-called readily releasable pool of granules has been described in rodent β-cells and β-cell-derived lines; it is discharged by less exhaustive flash photolysis of caged Ca^{2+} compounds raising $[Ca^{2+}]_i$ to between >0.5 and <5 μM and is called a highly Ca sensitive pool (HCSP).[6] This is precisely the range of $[Ca^{2+}]_i$ that (i) induces similar slow rates of continuous exocytosis in β-cells either dialyzed via whole cell patching with pipettes containing buffered Ca^{2+} solutions[2,7] or permeabilized to extracellular Ca^{2+} by the channel forming neurotoxin α-latrotoxin[9] and (ii) induces the slow rates of insulin secretion displayed by digitonin-permeabilized β-cells.[19] The size of the HCSP is greatly augmented by pre-treatment of the cell with pharmacological stimulators of protein kinases A and C or by raising the ambient concentration of glucose but remains largely intact after a bout of repetitive stimulation that depletes the IRP.[6] In preliminary experiments with single human β-cells displaying only the tonic pattern of exocytosis we were able to identify a corresponding HCSP.[10] In the experiments we report here, where β-cells were exposed to enhancement of PKA (by forskolin) and near stimulatory levels of glucose, it is likely that the HCSP was particularly enhanced in prominence. In fact, Figure 5 demonstrates that addition of a membrane permeable analog of cAMP dramatically recruits *tonic exocytosis* in response to repetitive depolarization, under conditions where previously it was hardly apparent.

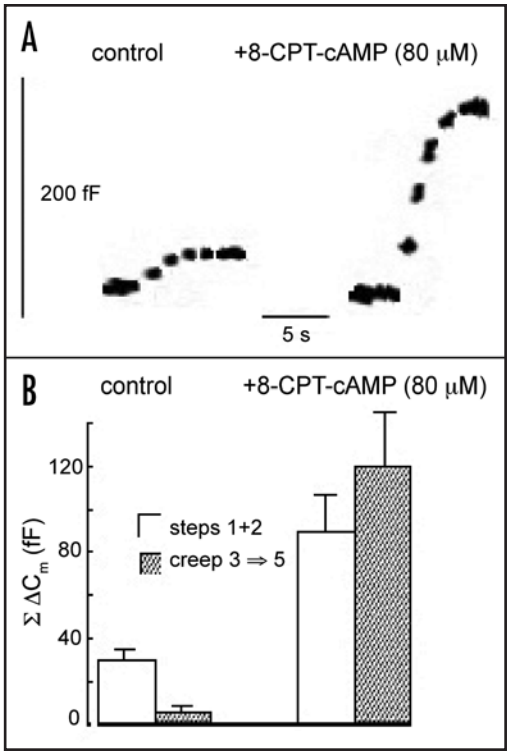

Figure 5. Enhancement of phasic exocytosis and revealing of tonic exocytosis in porcine β-cells by increases in $[cAMP]_i$. (A) shows that exposure of cells to 80 μM 8-CPT-cAMP enhances C_m steps after the initial 2–3 depolarizations in a train as well as recruits C_m creeps after the remaining depolarizations in the train. (B) shows that after 6 min incubation in 8-CPT-cAMP five cells displayed on average a 3-fold increase in the sum of the C_m steps seen in response to the first two depolarizations in the train, as well as a near 20-fold increase in the total C_m creep seen over the remainder of the depolarization train.

Figure 6 presents a summary schematic for the relative contributions of phasic and tonic modes of exocytosis (and their presumed sources, the IRP and HCSP respectively) to the release of insulin granules evoked both during and after depolarizations of increasing duration that initially raise local $[Ca^{2+}]_i$ near the mouths of a cluster (or "hot spot") of voltage dependent Ca^{2+} channels to >20 μM. As the duration of the depolarization increases, continuing Ca^{2+} entry produces an expanding domain of submembrane increase in $[Ca^{2+}]_i$. Within several ms of the start of Ca^{2+} entry, the diffusing Ca^{2+} is able to trigger exocytosis of granules of the IRP that are docked within nanometers of the Ca^{2+} channel "hot spot" and bind Ca^{2+} with a relatively low affinity. This produces the "step" increase in C_m seen after depolarization, where the step size is a function of duration of depolarization. When Ca^{2+} channels continue to remain open, within 10 s of ms the continually entering Ca^{2+} diffuses far enough so that a much lower concentration reaches, and hence triggers exocytosis from, granules of the HCSP, which, though docked far from Ca^{2+} channel "hot spot", bind Ca^{2+} with a relatively higher affinity. On cessation of Ca^{2+} current, the peak of $[Ca^{2+}]_i$ near the

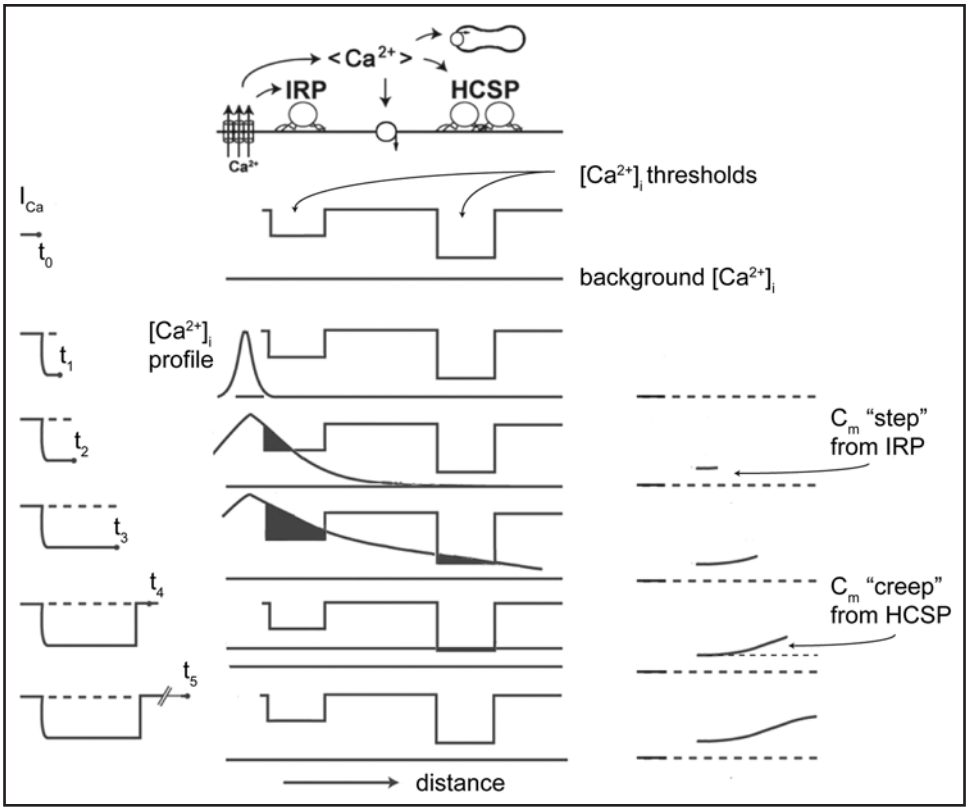

Figure 6. Schematic depiction of processes underlying phasic vs. tonic components of exocytosis in porcine β-cells. Increasing duration of depolarization-evoked Ca^{2+} current, promotes more prolonged Ca^{2+} entry and widens the profile of elevation $[Ca^{2+}]_i$. Beginning from background $[Ca^{2+}]_i$ present at t_0, a very brief depolarization extending to t_1 (or brief action potential, not shown) transiently raise local $[Ca^{2+}]_i$ over a small submembrane domain very near these Ca^{2+} channels. With a longer depolarization extending to t_2 (or with a longer duration action potential), the spreading profile of elevated $[Ca^{2+}]_i$ exceeds the threshold for initially activating an immediately releasable pool (IRP) of insulin granules docked near a cluster of high voltage activated Ca^{2+} channels. This produces phasic exocytosis, seen as a C_m step. With further extension of the depolarization to t_3 (or with a train of high frequency action or an action potential giving way to a plateau depolarization), the tail of spreading profile of elevation $[Ca^{2+}]_i$ exceeds the threshold for initially activating a highly Ca^{2+} sensitive pool (HCSP) of insulin granules far from Ca^{2+} channels. This produces tonic exocytosis or subsequent C_m "creep" following the phasic exocytosis or C_m step. Further prolongation of the depolarization gradually raises $[Ca^{2+}]_i$ over the entire non-organelle cytoplasm further extending the intensity and duration of the C_m "creep". The rise in $[Ca^{2+}]_i$ persists for up to seconds after the cessation of Ca^{2+} entry (e.g., to t_4) or until organelle Ca^{2+} uptake and plasma membrane Ca^{2+} extrusion mechanisms reduce local $[Ca^{2+}]_i$ to background levels. Hence release from the HCSP may contribute to tonic exocytosis, presenting as prolonged C_m "creep" until the profile of elevation $[Ca^{2+}]_i$ collapses back to background $[Ca^{2+}]_i$ levels (e.g., at t_5).

Ca^{2+} channel "hot spot" rapidly collapses to levels below where it is able to trigger exocytosis from IRP. However, the local $[Ca^{2+}]_i$ at some distance from the hot spot is likely to remain elevated and exceed the threshold for triggering release from the HCSP for up to seconds thereafter (i.e., until intracellular and plasma membrane Ca^{2+} transporters re-establish Ca^{2+} homeostasis). This produces the slower, more continuous "creeping" rise in C_m seen after the step increase in C_m under conditions of prolonged depolarization. Given this model it is not unreasonable to predict that plateau depolarizations (PDs) to V_ms insufficient to raise discrete submembrane hot spots of Ca^{2+}_i to values that evoke phasic release from IRP, if prolonged over several seconds, might still contribute enough distributed Ca^{2+} entry to generate a broad Ca^{2+}_i domain and evoke tonic release from HCSP. Similarly, prolonged, second messenger-induced release of Ca^{2+} from submembrane intracellular stores might trigger exocytosis from the HCSP.

Two important limitations to our data are worth defining. *First*, as the islet tissue we used consisted of small clumps or strands of cells we can only extrapolate our data to the electrical activity of β-cells in fully intact porcine islets. We suggest that it is likely that in the intact porcine islet β-cells are electrically coupled and exposed to incretins and glucagon, as they are in islets of other species[21] and that this would allow them to exhibit more electrical activity than that seen under our experimental conditions where we recorded from isolated cells mostly in the absence of $[cAMP]_i$ enhancers (e.g., Fig. 4). Given that (i) electrical coupling synchronizes the electrical activity while appearing to leave the morphology of individual action potentials intact, and (ii) $[cAMP]_i$ enhance the development of electrical activity at most levels of $[glucose]_o$, we suggest it is likely that in vivo *phasic exocytosis* would be enhanced over our experimental conditions. Given that higher action potential frequency predisposes to inactivation of Na currents, intact porcine islets would be more susceptible to developing plateau depolarizations and thus have greater opportunities for *tonic exocytosis*. Furthermore, our data from single cells (Fig. 5) would suggest that appropriately timed appearance of incretins and paracrine hormones, which increase $[cAMP]_i$ and perhaps release Ca^{2+} from intracellular stores, should directly or indirectly increase the sizes of the IRP as well HCSP, and hence further enhance phasic as well as tonic exocytosis. *Second*, unfortunately our data does not allow us to directly comment on either (i) the timing of exocytotic release of insulin in either the phasic or tonic release mode (i.e., whether insulin is released as rapidly as C-peptide[22]) or (ii) the precise timing of granule membrane endocytosis (e.g., rapid kiss-and-run mode of fusion/fission[23]).

The joint contribution of both *tonic and phasic exocytosis* to quantal release during sustained activity is a well appreciated phenomenon in excitable cells. First observed at the neuromuscular junction as (i) increased miniature endplate potential activity

interspersed between individually evoked endplate potentials[24,25] and (ii) as sustained miniature endplate potential frequency during nerve terminal depolarizations that do not trigger action potentials,[26] it has more recently been seen in the outputs of rapidly firing central inhibitory interneurons[27] and as well as the adrenal chromaffin cells driven by a train of action potentials.[28] Also, time courses of increases in C_m, very similar to what we define as phasic and tonic, have previously been reported from peptidergic neurophypohyseal terminals and adrenal chromaffin cells, though these results were interpreted in a different fashion.[29,30] It is worth noting that the adrenal chromaffin cell also has clearly definable IRP and HCSP.[31] In the chromaffin cell, synaptotagmin-1 (syt-1), the canonical synaptotagmin isoform identified as the Ca^{2+} sensor for fast synchronous exocytosis forebrain neurons, appears to be the sensor for phasic exocytosis, while an alternative isoform, syt-7, appears to be an important Ca^{2+} sensor for tonic exocytosis.[32] In β-cells, the situation is less clear: while the role of syt-1 is unclear, there is new evidence of impaired insulin secretion (second phase >first) in syt-7 null mutant mice and their β-cells.[33]

We propose that both the phasic and tonic patterns of exocytosis may be consistent phenomenon in large, long-lived mammals, including humans, and both modes of exocytosis and may play a role in determining the exact kinetics of insulin secretion.[11] Perhaps the most intriguing possibility for discrete and important roles for each mode of exocytosis, as well as their augmentation by increases in $[cAMP]_i$, occurs in canine islets where the biphasic glucose-induced insulin-secretion is (i) highly dependent on the presence of an enhancer of $[cAMP]_i$ and (ii) its time course closely resembles the combined time courses of the two phases of its biphasic electrical activity. Specifically, the brief *initial, or spike*, phase of insulin secretion greatly reduced by TTX, correlates well in time with a phase of single β-cell electrical activity largely consisting of Na^+ upstroke action potentials while the extended *second, or dome*, phase of insulin secretion correlates in time with an ongoing plateau depolarization to ~-20 to -25 mV.[34] Our ongoing investigations of single canine β-cells show (i) that single or brief trains of action potentials produce "phasic exocytosis" while plateau depolarizations produce "tonic exocytosis" and (ii) that each mode is appropriately modulated by glucose-dependent processes to shape a time dependence of single cell exocytosis mirroring the time course of insulin release from a population of perifused canine β-cells.[35]

Methods

The methods used in this study, including perforated patch electrophysiology, cytosolic Ca measurements and single cell assays of exocytosis, were identical to those described in our companion survey study characterizing electrophysiological properties of porcine β-cells,[12] and are direct applications of those used for the study of human and canine β-cells.[9,10] In experiments where exocytosis was directly measured, forskolin (10 μM) was added to the appropriately modified physiological saline solution (PSS), to increase the efficiency of coupling of depolarization to secretion without interfering with electrochemical detection of exocytotic release of insulin granule contents.[2,12] To record whole-cell currents simultaneously with membrane capacitance, patch pipettes were filled with high Cs^+ internal solution (Cs^+-IS) containing, in mM: 63.7 CsCl; 28.35 Cs_2SO_4; 47.2 sucrose; 11.8 NaCl; 1 $MgCl_2$; 0.5 mM EGTA and 20 HEPES titrated to pH 7.35 with NaOH. In experiments where glucose-induced electrical activity was recorded, an alternative high K^+ internal solution (K^+-IS), in which K^+ replaced Cs^+ on a mole-for-mole basis, was used. As discussed in the companion paper,[11] the cells chosen for study by single cell electrical, electrochemical and calcium imaging techniques were the largest single cells seen (>12 μm in diameter and >5.5 pF in baseline cell capacitance), criteria previously used to identify β-cells in other species and supported by our limited recordings from smaller cells, which displayed features more characteristic of α-cells in other mammalian species. Current-clamp recording was begun after the pipette-to-cytoplasm access resistance (R_a) fell to <40 M while voltage clamp recording was begun after R_a fell to <30–25 MΩ, with the cell initially stepped from a holding potential of -70 mV. Whole cell currents were leak subtracted using a standard p/4 protocol. Quantal release events (QREs) were monitored by amperometry using a carbon fiber electrode (tip potential = +650 mV) positioned at the surface of cells that were previously loaded with serotonin (5-HT) and 5-hydroxytryptophan, at incubation concentrations of 0.5 mM each, and then bathed in a PSS containing 4 mM glucose and 10 μM forskolin that was maintained at 32°C. Membrane capacitance changes (ΔC_m) following cell depolarization were estimated using an EPC-9 patch clamp amplifier (Heka, Electronic, Lambrecht, Germany) and software-based, dual frequency lock-in detector (LID) developed as a set of extensions (XOP modules) of the numerical/graphics package Igor (Wavemetrics, Inc., Oregon, USA) to (i) apply dual-frequency, small signal voltage excitation (10 mV peak-to-peak at 400 and 800 Hz) to the cell held at a DC potential of -70 mV and (ii) subsequently process the current response.

Acknowledgements

We thank (i) Human Islet Transplantation Laboratory, Washington University Medical Center, especially Barbara Olack and Carole Swanson, for the provision of islets; (ii) June Liu-Gentry for participation in early experiments; and (iii) Alon Friedman, Advanced Teacher Training Center at Shlomi, Israel for expert help with design and execution of several of the figures. This work was principally supported by grants from the National Institutes of Health 4RO1-DK37380 to Stanley Misler and ROI-DK20579 to M. Mohanakumar (Dept. of Surgery, Washington University in St. Louis) for isolation of islets. Additionally, Amelia M. Silva was partially supported by a grant from the Luso-American Foundation of Portugal and Adam S. Dickey was supported by a National Institutes of Health Medical Scientist Training Grant (5T32 GM07281) to the University of Chicago.

References

1. Gillis KD, Misler S. Single cell assay of exocytosis from pancreatic islet β cells. Pfluegers Arch 1992; 420:121-3.
2. Ammala C, Eliasson L, Bokvist K, Larsson O, Ashcroft FM and Rorsman P. Exocytosis elicited by action potentials and voltage-clamp calcium currents in individual mouse pancreatic beta-cells. J Physiol 1993; 472:665-88.
3. Zhou Z and Misler S. Amperometric detection of quantal secretion from patch-clamped rat pancreatic β-cells. J Biol Chem 1996; 271:270-7.

4. Huang L, Shen H, Atkinson MA, Kennedy RT. Detection of exocytosis at individual pancreatic β-cells by amperometry at a chemically modified microelectrode. Proc Natl Acad Sci USA 1995; 92:9608-12.
5. Barg S, Ma X, Eliasson L, Galvanovskis J, Gopel SO, Obermuller S, et al. Fast exocytosis with few calcium channels in insulin-secreting mouse pancreatic B cells. Biophys J 2001; 81:3308-23.
6. Barg S, Eliasson L, Renström E, Rorsman P. A subset of 50 secretory granules in close contact with L-type Ca^{2+} channels accounts for first-phase insulin secretion in mouse beta-cells. Diabetes 2002; 51:74-82.
7. Yang Y, Gillis KD. A highly Ca^{2+}-sensitive pool of granules is regulated by glucose and protein kinases in insulin-secreting INS-1 cells. J Gen Physiol 2004; 124:641-51.
8. Barnett DW, Misler S. Coupling of exocytosis to depolarization in rat pancreatic islet beta-cells: effects of calcium, strontium and barium containing extracellular solutions. Pfluegers Arch 1995; 430:593-5.
9. Misler S, Dickey A, Barnett DW. Maintenance of stimulus-secretion coupling and single beta-cell function in cryopreserved-thawed human islets of Langerhans. Pfluegers Arch 2005; 450:395-404.
10. Silva AM, Liu-Gentry J, Dickey AS, Barnett DW and Misler S. α-Latrotoxin increases spontaneous and depolarization-evoked exocytosis from pancreatic islet β-cells. J Physiol 2005; 565:783-99.
11. Misler S, Barnett DW, Gillis KD. Update on Electrophysiology of Stimulus-Secretion Coupling in Human β Cells. In "Retrospectives on Prospectives in Diabetes", Robertson RP, ed 2006.
12. Silva AM, Dickey AS, Barnett DW, Misler S. Ion channels underlying stimulus-exocytosis coupling and its cell-to-cell heterogeneity in β-cells of porcine islets of Langerhans (companion MS submitted to Channels) 2009.
13. Barnett DW, Pressel DM, Chern HT, Scharp DW, Misler S. cAMP-enhancing agents "permit" stimulus-secretion coupling in canine pancreatic islet beta-cells. J Membrane Biol 1994; 138:113-20.
14. Grynkiewicz G, Poenie M, Tsien RY. A new generation of Ca^{2+} indicators with greatly improved fluorescence properties. J Biol Chem 1985; 260:3440-50.
15. Borst JGG, Sakmann B. Effect of changes in action potential shape on calcium currents and transmitter release in the calyx-type synapse of the rat auditory brainstem. Phil Trans Royal Soc Lond. B 1999; 354:347-55.
16. Ammala C, Ashcroft FM, Rorsman P. Calcium independent potentiation of insulin releaseby cyclic AMP in single β-cells. Nature 1993; 363:356-8.
17. Gillis KD, Misler S. Enhancers of cytosolic cAMP augment depolarization-induced exocytosis from pancreatic B-cells: evidence for effects distal to Ca^{2+} entry. Pfluegers Arch 1993; 424:195-7.
18. Gromada J, Bokvist K, Ding WG, Holst JJ, Nielsen JH, Rorsman P. Glucagon-like peptide 7–37 amide stimulated exocytosis in human pancreatic beta-cells by both proximal and distal regulatory steps in stimulus-secretion coupling. Diabetes 1998; 47:57-65.
19. Augustine GJ, Neher E. Calcium requirements for secretion in bovine chromaffin cells. J Physiol 1992; 450:247-71.
20. Jones PM, Persuad SJ, Howell SL. Calcium-induced insulin secretion from electrically permeabilized islets. Biochem J 1992; 285:973-8.
21. Zhang Q, Galvanovskis J, Abdulkader F, Partridge CJ, Gopel SO, Eliasson L, Rorsman P. Cell coupling of mouse β-cells measured in intact islets of Langerhans. Phil Trans Royal Soc A 2008; 366:3503-23.
22. Michael DJ, Ritzel RA, Haataja L, Chow RH. Pancreatic β-cells secrete insulin in fast and slow release forms. Diabetes 2006; 55:600-7.
23. Hanna ST, Pigeau GM, Galvanovskis J, Clark A, Rorsman P, MacDonald PE. Kiss-and run exocytosis and fusion pores of secretory vesicles of human β-cells. Pfluegers Arch 2008; (in press, on line publication).
24. Liley AW. The quantal components of the mammalian end-plate potential. J Physiol 1956; 133:571-87.
25. Hurlbut WP, Longenecker HB, Mauro A. Effects of calcium and magnesium on the frequency of miniature end-plate potentials during prolonged tetanization. J Physiol 1971; 219:17-38.
26. Liley AW. The effects of presynaptic polarization on the spontaneous activity at the mammalian neuromuscular junction. J Physiol 1956; 134:427-43.
27. Zhou Z, Misler S. Action potential-induced quantal secretion of catecholamines from rat adrenal chromaffin cells. J Biol Chem 1995; 271:3498-505.
28. Heft S, Jonas P. Asynchronous GABA release generates long-lasting inhibition at a hippocampal interneron-principal neuron synapse. Nature Neuroscience 2005; 8:1319-28.
29. Seward EP, Chernevskaya NI, Nowycky MC. Exocytosis in peptidergic nerve terminals exhibits two Ca-sensitive phases during pulsatile calcium entry. J Neurosci 1995; 15:3390-9.
30. Seward EP, Nowycky MC. Kinetics of stimulus-coupled secretion in dialyzed bovine chromaffin cells in response to trains of depolarizing pulses. J Neurosci 1996; 16:553-62.
31. Yang Y, Udayasankar S, Dunning J, Chen P, Gillis KD. A highly Ca^{2+} sensitive pool of vesicles is regulated by protein kinase C in adrenal chromaffin cells. Proc Natl Acad Sci USA 2002; 99:17060-5.
32. Schonn J-S, Maximov A, Lao Y, Sudhof TC, Sorensen JB. Synaptotagmin-1 and -7 are functionally overlapping Ca^{2+} sensors for exocytosis in adrenal chromaffin cells. Proc Natl Acad Sci USA 2008; 105:3998-4003.
33. Gustavsson N, Lao Y, Maximox A, Chuang J-C, Kostromina Repa JA, Li C, et al. Impaired insulin secretion and glucose tolerance in synaptotagmin-7 null mutant mice. Proc Natl Acad Sci USA 2008; 105:3992-7.
34. Pressel DM, Misler S. Role of voltage dependent ionic currents in coupling glucose stimulation to insulin secretion in canine pancreatic islet β-cells. J Membrane Biol 1991; 124:239-53.
35. Misler S, Dickey A, Silva AM, Pressel D and Barnett DW. Correlates of biphasic insulin secretion in single cell exocytosis by canine β-cells. Diabetes 2004; 53:393.